CDK6 ACTIVITY IN A RECURRING CONVERGENT KINASE NETWORK MOTIF

Christina Gangemi[a,b], Rahkesh T Sabapathy[c] & Harald Janovjak[a,b,c]

[a] Australian Regenerative Medicine Institute (ARMI), Faculty of Medicine, Nursing and Health Sciences, Monash University, 3800 Clayton/Melbourne, Victoria, Australia

[b] European Molecular Biology Laboratory Australia (EMBL Australia), Monash University, 3800 Clayton/Melbourne, Victoria, Australia

[c] Flinders Health and Medical Research Institute, College of Medicine and Public Health, Flinders University, 5042 Bedford Park/Adelaide, South Australia, Australia

To whom correspondence should be addressed: harald.janovjak@flinders.edu.au.

Keywords: Kinase, signaling network, inhibitor, protein engineering, convergence

ABSTRACT

More than 500 kinases phosphorylate ~15% of all human proteins. The global architecture of the phosphorylation network has been studied extensively, for instance to compile comprehensive interaction maps, trace signal transduction pathways or identify chemical intervention points. In contrast, systematic investigation of local motifs is rarer but may provide a complementary understanding of network features and kinase function. Here, we report on the occurrence, topology and experimental analysis of convergent kinase-substrate relationships (cKSRs). cKSRs are motifs in which ≥two kinases phosphorylate the same substrate. Through bioinformatics analysis of phosphorylation site maps we found that cKSRs are frequent and involve >80% of all human kinases and >24% of all substrates. We show that cKSRs occur over a wide range of stoichiometries and that groups of converging kinases are in many instances co-expressed. Experimentally, we demonstrate for the prototypical convergent CDK4/6 kinase pair how multiple inputs at the major tumor suppressor retinoblastoma protein (RB) can hamper *in situ* analysis of individual kinase functions. We hypothesized that overexpression of one kinase combined with a CDK4/6 inhibitor can dissect convergence. In breast cancer cells that express high levels of CDK4, we confirmed this hypothesis and developed a high throughput compatible assay that sensitively quantifies genetically modified CDK6 variants, small molecule inhibitors and inhibitory protein interactions. Collectively, our work provides deeper insight into the phosphorylation network by revealing fundamental properties of cKSRs and demonstrates a strategy to study these recurring motifs in cellular environments.

INTRODUCTION

Protein phosphorylation is the most common reversible post-translational modification in eukaryotes and an essential regulator of cell and organism physiology in health and disease. Recent experimental analysis of the phosphoproteome has revealed a large number of human protein phosphorylation sites (e.g., >200'000 sites in large mass spectrometry-based datasets, or >10'000 sites with experimentally validated kinase-substrate interactions) (Aebersold and Mann, 2016; Colinge et al., 2014; Hornbeck et al., 2015; Lemeer and Heck, 2009; Riley and Coon, 2016). The architecture of the emerging phosphorylation network has been studied extensively. Whilst many studies focused on global interaction maps or linear/interconnected signaling pathways (reviewed in (Alganem et al., 2022; Chen and Eschrich, 2014; Colinge *et al.*, 2014)), less attention has been devoted to a network-wide analysis of local motifs (Invergo and Beltrao, 2018). With ~500 kinases and ~3'000 substrate proteins encoded in the human genome, it is expected that each kinase phosphorylates many sites and that on each substrate protein multiple sites are phosphorylated. Nodes in which multiple kinases converge on one substrate (**Fig. 1A, left**) are likely to occur in the network but their number and topologies have not been systematically investigated. Convergent network motifs are of interest not only because of their involvement in biological functions, including signal amplification, pathway crosstalk and feedback loops (**Fig. 1A, right**), but also because they can lead to challenges during experimental interrogation. For instance, quantifying the activity of a kinase *in situ* can be hampered by background phosphorylation of its substrate by additional convergent kinases. Indeed, in well-known cases of convergence, the presence of multiple inputs has resulted in limited experimental methods for functional analysis (see below).

One prototypical case of phosphorylation convergence centers around the CDK4/6 serine (Ser)/threonine (Thr) kinase pair. CDK4/6 and their associated D-type cyclins (CyclinD1/D2/D3) are core components of the cell cycle machinery and regulate commitment to cycle entry (Malumbres and Barbacid, 2001; Sherr and Roberts, 1999). Unbound CDK4/6 are catalytically inactive. Assembled active CDK4/6-D-type cyclin complexes are regulated positively (e.g., by the CDK-activating complex (Fisher, 2005; Schachter et al., 2013)), negatively (e.g., by INK4 proteins (Hirai et al., 1995; Parry et al., 1999; Sherr and Roberts, 1999)), as well as positively or negatively in a context dependent manner (e.g., by KIP proteins (Blain, 2008; Cheng et al., 1999; Parry *et al.*, 1999; Sherr and Roberts, 1999)). Within the cell cycle, CDK4/6 phosphorylate key regulatory sites on the major growth suppressor RB (Kaelin, 1999; Rubin, 2013). RB scavenges E2F transcription factors that are required for cell cycle progression and phosphorylation by various cyclins releases this interaction. Whilst their roles in the cell cycle and in many cases their substrate specificity are overlapping (Malumbres et al., 2004), CDK4/6 also have non-overlapping kinase activity-dependent and -independent functions outside of the cell cycle (Anders et al., 2011; Dall'Acqua et al., 2017; Hydbring et al., 2016; Tigan et al., 2016; Wang et al., 2017). Not surprisingly, CDK4/6 have received attention as major drivers of cancer and are targeted using small molecule inhibitors (Malumbres, 2014; Sherr et al., 2016). However, the absence of inhibitors that are specific for either kinase and their overlapping activity can challenge experimental analysis.

As shown previously, the presence of either CDK4 or CDK6 is sufficient to phosphorylate RB to levels that prohibit analysis of the activity of the other kinase (Malumbres *et al.*, 2004; Yang et al., 2017). As a consequence, CDK4 and CDK6, in particular in the context of RB phosphorylation, are commonly functionally assayed *in vitro,* either using purified kinases and substrates, such as a recombinant RB fragment (Bockstaele et al., 2006; Jinno et al., 1999; Kitagawa et al., 1996; Paternot et al., 2003), or after immunoprecipitation (Bockstaele et al., 2009; Bockstaele *et al.*, 2006). More recently, fluorescent biosensors of CDKs were developed but these require substrate-specific chemically-functionalized polypeptide probes and have not been deployed in living cells (Pellerano and Morris, 2021; Soamalala et al., 2020; Van et al., 2014). In cells, large scale exploration of potential CDK6 substrates was conducted using gel-based

electrophoretic migration shift assays that do not offer high throughput and may not in all cases provide the resolution required to visualize phosphorylation events (Anders *et al.*, 2011). Finally, transcriptional reporter plasmids for signals downstream of RB often exhibit low signal-to-noise ratios (Budde et al., 2005; Chen et al., 1996a; Chen et al., 1996b). Collectively, assaying the CDK4/6-RB-axis in complex cellular environments and compatible with parallelization is currently challenging. Because of its biological/biomedical significance and these experimental limitations, the CDK4/6 pair represents an interesting test case for experimental convergence analysis.

Here, we first performed a network-wide analysis of local kinase-substrate interactions with a focus on cKSRs. We quantified their frequency and topology. We then hypothesized that kinase overexpression combined with the use of a CDK4/6 inhibitor provides an approach to assay an individual kinase of the pair. Using this strategy, we were able to characterize genetically modified CDK6s and their inhibitors in breast cancer cells expressing high levels of CDK4. Collectively, our work reveals fundamental properties of cKSRs and demonstrates a possible approach to dissect convergence in cellular contexts even in the absence of kinase-specific inhibitors.

MATERIALS AND METHODS

Key resources table

REAGENT or RESOURCE	SOURCE	IDENTIFIER
Reagents		
Abemaciclib (LY2835219)	AdooQ Bioscience	A12989
Ribociclib (LEE011)	Selleckchem	S7440
MEM	Gibco	11095080
Penicillin streptomycin	Gibco	15140122
FBS	Gibco	26140079
Insulin, recombinant human zinc solution	Gibco	12585014
PBS	Gibco	20012050
Opti-MEM	Gibco	31985070
X-tremeGENE HP DNA Transfection Reagent	Roche	6366236001
Cell Lysis Buffer (10X)	Cell Signalling Technology	9803S
Glycerol	Sigma-Aldrich	G5516-500ML
SDS	Sigma-Aldrich	L3771-500G
Bromophenol blue	Sigma-Aldrich	B0126-25G
β-mercaptoethanol	Sigma-Aldrich	M3148-25ML
20X Bolt MOPS SDS Running Buffer	Invitrogen	B0001
Bolt 4-12% Bis-Tris Plus Gels 15-well	Invitrogen	NW04125BOX
Immun-Blot PVDF Membrane	Bio-Rad	1620177
BSA	Sigma-Aldrich	A7906-50G
Tween 20	Sigma-Aldrich	P1379
Clarity Western ECL Substrate	Bio-Rad	1705060
Antibodies		
DYKDDDDK Tag (D6W5B) Rabbit mAb (FLAG-Tag)	Cell Signaling Technology	14793

GAPDH (D16H11) XP Rabbit mAb	Cell Signaling Technology	5174
HA-Tag (C29F4) Rabbit mAb	Cell Signaling Technology	3724
Phospho-RB (Ser780) (D59B7) Rabbit mAb	Cell Signaling Technology	8180
RB (4H1) Mouse mAb	Cell Signaling Technology	9309
Goat Anti-Mouse IgG (H+L)-HRP Conjugate	Bio-Rad	1721011
Goat Anti-Rabbit IgG (H + L)-HRP Conjugate	Bio-Rad	1706515
Kits		
AlphaLISA SureFire Ultra p-RB (Ser780)	PerkinElmer	ALSU-PRB-C
AlphaLISA SureFire Ultra RB Total	PerkinElmer	ALSU-TRB-A

KSR analysis

The KSR analysis was based on a comprehensive set of experimentally determined phosphorylation sites deposited in PhosphoSitePlus (PSP) (Hornbeck *et al.*, 2015). PSP is continuously manually-curated. Phosphorylation sites were downloaded (http://www.phosphosite.org; v6.6.0.2, February 2022) and further processed to obtain cKSRs using custom macros and formulas.

The first analysis was substrate-centric. This analysis was performed for Ser/Thr and tyrosine (Tyr) phosphorylation events separately and by considering either *general* cKSRs (i.e., ≥two kinases phosphorylate the same substrate but not necessarily at the same site) or *site-specific* cKSRs (i.e., ≥two kinases phosphorylate the same substrate at the same phosphorylation site). First, PSP sites were limited to human substrate entries. Second, to eliminate duplicate pairings of kinases and substrates/sites for accurate counting, fingerprints were calculated that combined the kinase and substrate/site name (e.g., “CDK4:RB” or “CDK4:RB:S780”). In a third step, the fingerprints were used to identify unique substrates/sites. In a fourth step and for each unique substrate/site, the number of active kinases was counted and their names compiled. For general cKSRs, these unique lists are given in **Supplementary Tables S1 and S2** (Ser/Thr and Tyr phosphorylation, respectively). For site-specific cKSRs, these unique lists are given in **Supplementary Tables S3 and S4** (Ser/Thr and Tyr phosphorylation, respectively). Finally, the occurrence of each possible cKSR of K:1 topology (where K denotes the number of kinases and is between 1 and 50, and 1 denotes the substrate/site) were counted. This analysis also reported on the total number of substrates/sites involved in cKSRs.

The second analysis was kinase-centric. This analysis was performed for Ser/Thr and Tyr kinases separately. Above kinase-substrate pairings were reanalyzed to produce filtered lists of kinases. The main applied filter was to include only those kinases which phosphorylate substrates that are subject to general or site-specific cKSRs (**Supplementary Tables S5-S8**). This list was then further used to retrieve kinase-specific information, such as the number of substrates that is phosphorylated by each kinases.

Co-expression analysis

The co-expression analysis was based on an analysis of 1393 cancer cell lines collected by the cancer cell line encyclopedia initiative (Barretina et al., 2012). Expression data of all protein-coding genes in the $\log_2$(TPM+1) format (where +1 denotes a pseudocount) were downloaded (v22Q1, April 2022, http://sites.broadinstitute.org/ccle/, http://depmap.org/portal/download/) and further processed using custom macros and formulas. This analysis was performed for Ser/Thr and Tyr phosphorylation events separately and by considering either general or site-specific

cKSRs. First, protein names in the expression data were cropped to only contain short HGNC compliant names. Second, the TPM values were converted into a binary format (1: expressed, 0: not expressed) using specified TPM thresholds (5, 10 and 20). Third, lists containing the names of kinases phosphorylating each substrate/site were generated (as in **Supplementary Tables S1-S4**). Where necessary and in a small number of cases, kinase nomenclature was corrected using the nomenclature list of KinHub (http://kinhub.org). Fourth, for each group of kinases that act on a substrate/site, the number of cell lines was counted in which ≥two convergent kinases are co-expressed. The percentage was defined as the co-expression score.

Reagents

Reagents utilized are listed in the Key Resources Table. Abemaciclib (LY2835219) (AdooQ Bioscience) was diluted in dimethyl sulfoxide (DMSO) to generate a 2 mM stock solution. Ribociclib (LEE011) (Selleckchem) stock solutions were prepared at 10 mM in DMSO. Inhibitors were further diluted in cell culture media before being added to cells and equivalent amounts of DMSO were added to control wells.

Vectors and constructs

All genes were ordered as synthetic genes (gBlocks, Integrated DNA Technologies) and designed to contain an N-terminal HA-tag (YPYDVPDYA), with the exception of Cyclin D3 that contained an N-terminal FLAG-tag (DYKDDDDK). gBlocks were amplified in polymerase chain reactions using oligonucleotides with restriction site overhangs and digested with the corresponding restriction enzymes. These were NotI and BamHI for wildtype (WT) CDK6 and p18INK4a, XhoI and BamHI for Cyclin D3, NotI and BstEII for CDK6 with N-terminal pdDronpa1, and BstEII and BamHI for CDK6 with internal loop pdDronpa1 (New England Biolabs). pcDNA3.1(-) vector (Thermo Fisher Scientific) was digested with the corresponding enzymes and ligated with amplified genes using T4 DNA ligase (Promega).

Single residue mutations were introduced in WT CDK6 using overlapping oligonucleotides designed in PrimerX (https://www.bioinformatics.org/primerx/) using the QuikChange option. Circular PCRs were performed with a high-fidelity polymerase (Q5, NEB) followed by digestion with DpnI restriction enzyme (New England Biolabs).

All genes were verified using Sanger sequencing (MicroMon, Monash University). The sequences of the engineered CDK6 fusion proteins are summarized in **Supplementary Table S9.**

Cell culture

Human breast cancer MCF-7 cells (ATCC, HTB-22) were kindly provided by Antonella Papa (Monash University) and cultured in Minimum Essential Media (MEM, Gibco) in a humidified incubator with 5% CO_2 atmosphere at 37°C. Medium was supplemented with 10% FBS, 0.1 mg/ml human recombinant insulin, 100 U/ml penicillin and 0.1 mg/ml streptomycin (Gibco). Transfections were conducted by seeding 500,000 cells per well in 6-well plates for immunoblotting experiments or 18,000 cells in 96-well plates for AlphaLISA assays. 24 hrs after seeding, cells were transfected with plasmid DNA using X-tremeGENE HP DNA transfection reagent (Roche) as per the manufacturer's protocol using a total vector amount of 2 µg (6-well) or 0.1 µg (96-well). A 3:1 ratio of transfection reagent to DNA; (6 µl:2 µg) for 6-well or (0.3 µl:0.1 µg) for 96-well was used. Single construct controls were supplemented with empty pcDNA3.1(-) vector and for co-expression plasmids were added in a ratio of 1:1 or 1:1:1. Mock transfections contained empty pcDNA3.1(-) vector only. After 24 hrs, the culture medium was replaced and CDK4/6 inhibitor/s added.

209 *Immunoblotting*

210 After 24 hrs of inhibitor treatment, cells were transferred onto ice and washed with cold 1x
211 phosphate-buffered saline (PBS). 500 µl of 1x cell lysis buffer (Cell Signalling Technology)
212 supplemented with Complete EDTA-free Protease Inhibitor Cocktail (Roche) was added for cell
213 lysis. Lysates were collected and sonicated for 10 s, followed by incubation at 4°C with constant
214 shaking (2000 rpm) for 30 min. Samples were then centrifuged for 20 min at 4°C before adding
215 4x Laemmli loading buffer (40% glycerol, 240 mM Tris/HCL, pH 6.8, 8% SDS, 0.04%
216 bromophenol blue and 5% β-mercaptoethanol) and denaturation at 95°C for 5 min. Proteins were
217 separated using Bolt 4-12% Bis-Tris Plus Gels (Invitrogen) run at 140 V for 60 min before being
218 transferred onto PVDF membranes (100 V for 100 min) (Bio-Rad). Membranes were blocked in
219 1x TBST (1x Tris-buffered saline, 0.1% Tween) containing 5% skim milk powder for >1 hr at room
220 temperature (rotating). Membranes were then probed with indicated primary antibodies (diluted
221 in either 5% skim milk powder or bovine serum albumin in 1x TBST) overnight whilst rotating at
222 4°C. Corresponding mouse or rabbit horseradish peroxidase-conjugated secondary antibodies
223 (diluted 1:10,000 in 1x TBST) were added for 1 hr at room temperature (Bio-Rad).
224 Chemiluminescence was detected by adding Clarity Western ECL Substrate (1:1 of luminol and
225 peroxide solutions) in a ChemiDoc Touch Imaging System (Bio-Rad).

226

227 *Energy transfer-based assays*

228 AlphaLISA SureFire Ultra assay kits (PerkinElmer) were used in a two-plate two-incubation assay
229 protocol for adherent cells according to manufacturer's instructions. Briefly, cells were washed
230 with 100 µl of PBS per well, followed by addition of 100 µl of 1x lysis buffer and incubated for 10
231 min on a plate shaker at 350 rpm. Lysate was transferred to light grey 384-well untreated
232 AlphaPlates (PerkinElmer) by adding 10 µl per well. Both kits were used to run both assays in
233 parallel on the same lysates from each condition. 5 µl of acceptor mix was added per well and
234 incubated for 1 hr in the dark followed by addition of 5 µl of donor mix (under low light conditions)
235 and incubated for a further hour in the dark. Wells were then read using a PHERAstar plate reader
236 (BMG). Each condition was assayed in triplicates per kit.

237

238 *Data analysis and statistics*

239 Densitometry analysis was performed on immunoblots using ImageLab 6.1 software (Bio-Rad).
240 Kinase-substrate topology analysis was performed using equations and filters in Microsoft Excel.
241 Co-expression analysis was performed using macros written in C in Igor Pro 6.22 (Wavemetrics).
242 Data for **Supplementary Fig. S3** was prepared in UniProt (http://www.uniprot.org, alignment of
243 human CDK5 and CDK6) and PyMOL 2.5 (Schrödinger; protein structures: PDB-ID 1JOW for
244 CDK6 and 1H4L for CDK5). All other data was analysed using Prism (9.0, GraphPad).

245

246

247 **RESULTS**

248 *Convergent motifs are abundant in Ser/Thr and Tyr phosphorylation*

249 We systematically analyzed convergent phosphorylation motifs. As the data source we utilized
250 the comprehensive PSP repository of experimentally determined phosphorylation sites (Hornbeck
251 *et al.*, 2015). >21'000 phosphorylation sites are deposited in PSP across all species, with human
252 being the most prominent substrate types (accounting for 13'916 or 64% of sites). We limited our
253 analysis to these human phosphorylation sites and separated Ser/Thr from Tyr kinase reactions.
254 Using a fingerprinting approach, we identified unique substrates and for each substrate compiled

255 the phosphorylating kinases (**Supplementary Tables S1-S4**). We found that convergent motifs
256 are common both in Ser/Thr and Tyr phosphorylation. Of the 2629 substrates of 350 Ser/Thr
257 kinases, 1268 (48%) are phosphorylated by more than one kinase (**Fig. 1B**). Similarly, in the case
258 of Tyr phosphorylation by 129 kinases, 422 (65%) of 649 substrates are phosphorylated by more
259 than one kinase (**Fig. 1C**). We next determined cKSR topologies expressed as K:1, where K
260 denotes the number of kinases and 1 denotes the substrate. We found that 21, 10 and 6.1% of
261 substrates are phosphorylated by two, three or four Ser/Thr kinases, and the remaining substrates
262 by varying kinase numbers (**Fig. 1B,C**). We also found that 19, 6.6 and 5.2% of substrates are
263 phosphorylated by two, three or four Tyr kinases, and the remaining substrates by varying kinase
264 numbers. Thus, cKSRs are not only generally abundant but also occur with broad topologies that
265 are comparable between Ser/Thr and Tyr phosphorylation. These results depict general cKSRs
266 in which ≥two kinases phosphorylate the same substrate but not necessarily at the same site. We
267 went on to extend the analysis to site-specific cKSRs in which the same site is phosphorylated.
268 Also in this case we observed common convergent motifs in that 1946 (24%) of 7987 Ser/Thr
269 sites or 344 (23%) of 1494 Tyr sites were phosphorylated by ≥two kinases (**Fig. 1D,E**). As for
270 general cKSRs, a wide range of topologies was observed. We found that 15, 4.7 and 1.7% of
271 substrates are phosphorylated by two, three or four Ser/Thr kinases, and 15, 3.8 and 2.6% of
272 substrates phosphorylated by two, three or four Tyr kinases. Collectively, these results indicate
273 that diverse cKSRs comprise a significant fraction of the human phosphoproteome as mapped in
274 the PSP.

275

276 *Most kinases phosphorylate cKSR substrates*

277 We next asked how many kinases participate in cKSRs and if some stoichiometries are more
278 common than others (e.g., are few kinases acting on many substrates, or are many kinases acting
279 on few substrates). We defined the kinases of interest as those that act on substrates that are
280 phosphorylated by ≥two kinases. We found that this criterion applied to a large fraction of all
281 kinases (87% or 421 of 479 kinases listed in PSP) (**Fig. 2A-D**). More specifically, of 350 Ser/Thr
282 kinases, 324 or 298 (92 or 85%) were identified to act on general or site-specific cKSR substrates
283 (**Fig. 2A,C**, **Supplementary Tables S5 and S7**). For 129 Tyr kinases, fractions were somewhat
284 lower but still indicated prominence (61 or 67% associated with general or site-specific cKSR
285 substrates; **Fig. 2B,D**, **Supplementary Tables S6 and S8**). We also found that kinase
286 stoichiometries were broadly distributed. Of the identified kinases, most phosphorylated a small
287 number of substrates whilst a small number of kinases acted on many substrates (**Fig. 2A-D**).
288 Collectively, these data indicate that covergent motifs involve a large number of kinases through
289 complex interactions.

290 Finally, we also asked if these kinases are co-expressed to relate to biological effects of
291 cKSRs. We analyzed current RNA-sequencing data from 1393 human cell lines deposited in the
292 DepMap portal and cancer cell line encyclopedia (Barretina *et al.*, 2012). Similarly to above, we
293 compiled lists of active kinases for either each cKSR substrate or each cKSR phosphorylation
294 site. We then examined expression levels of these kinases (TPM≥10 in **Fig. 2E**, and also TPM≥5
295 and 20 in **Supplementary Fig. S1**). As a score for co-expression in each kinase group, we
296 quantified in how many of the 1393 cell lines at least two convergent kinases are expressed (**Fig.
297 2E, left**). Cases of co-expression are generally frequent (**Fig. 2E, right**). On average for TPM≥10,
298 the identified Ser/Thr kinase groups are co-expressed in >1000 (or >70%) of the analyzed cell
299 lines. Furthermore, only a small number of groups (<4%) were co-expressed more rarely (in
300 <2.5% of cell lines). Similarly for Tyr kinases, on average the groups were co-expressed in >930
301 (or >68%) of the analyzed cell lines with <9% of the groups co-expressed more rarely. Albeit co-
302 expression is generally more prominent for Ser/Thr compared to Tyr kinases, these data
303 collectively indicate that not only are large numbers of kinases participating in cKSRs but also
304 that these kinases are in many cases co-expressed.

305

306 *Consequences of cKSRs in a prototypical kinase pair*

307 The above analysis points to a significant occurrence of cKSRs. This promoted us to explore the
308 consequences of convergence and to develop a strategy to dissect it for a prototypical kinase pair
309 in which specific inhibitors are unavailable. This kinase pair consists of CDK4 and CDK6, two
310 cyclin-dependent kinases that act on the major cell cycle regulator protein RB. We selected the
311 human breast cancer cell line (MCF-7) as the main experimental system as this cell type exhibits
312 high CDK4 levels and low CDK6 levels (TPM_{CDK4}: 170, TPM_{CDK6}: 0.39) (Parry *et al.*, 1999; Yang
313 *et al.*, 2017) and thus offers the possibility to supplement one kinase with the other. Untreated
314 MCF-7 cells exhibit high levels of phosphorylated RB (pRB, Ser780) attributable to CDK4 (**Fig.**
315 **3A,B**) (Li et al., 2022; Yang *et al.*, 2017). We tested whether overexpression of CDK6 can elevate
316 pRB levels but observed only a minimal effect (~1.1-fold) in transfected cells. We also examined
317 CDK6 variants harboring two activating mutations, S178P (Bockstaele *et al.*, 2009) or R31C (Hu
318 et al., 2011). The S178P mutant results in the cyclin-independent activation of CDK6 and thus
319 increased cyclin-dependent activity *in vitro* (Bockstaele *et al.*, 2009), whilst the R31C mutation
320 prevents the binding of INK4 protein inhibitors resulting in sustained kinase activity (Hu *et al.*,
321 2011). Both activating mutations, however, did not result in higher pRB levels compared to WT
322 CDK6 (**Fig. 3A,B**). To test the possibility that D-type cyclins are limiting effects of overexpressed
323 CDK6 (Lin et al., 2001; Parry *et al.*, 1999), we co-transfected Cyclin D3. This D-type cyclin was
324 chosen over D1 and D2 as it is known to promote high levels of kinase activity when in complex
325 specifically with CDK6 (Lin *et al.*, 2001; Parry *et al.*, 1999). Cyclin D3 overexpression resulted in
326 minor increases in pRB levels (~1.2-fold) (**Fig. 3C,D**). The same was observed for CDK6-S178P
327 and -R31C co-transfected with Cyclin D3 (~1.3- and 1.2-fold elevation, resp.) (**Fig. 3C,D**).
328 Collectively, these results indicate that overexpression of CDK6 in cells that exhibit high
329 background activity of the convergent CDK4 does not alter pRB levels.

330

331 *CDK4/6 inhibition to isolate CDK6 activity*

332 Abemaciclib (LY2835219 [LY]) is an inhibitor of CDK4 and CDK6 with similar half maximal
333 concentrations (IC_{50} 2.0 and 9.9 nM) (Fassl et al., 2022; Gelbert et al., 2014). Previous studies
334 have shown that treatment of MCF-7 cells with LY resulted in the emergence of drug resistance.
335 This resistance was attributed to amplified CDK6 levels resulting in altered cellular inhibitor
336 sensitivity (Cornell et al., 2019; Li *et al.*, 2022; Li et al., 2018; Yang *et al.*, 2017). Based on these
337 observations, we hypothesized that application of LY may reduce background pRB levels in MCF-
338 7 cells and that consequently overexpressed CDK6 may become functionally detectable. We first
339 treated the cells with 0.1 μM LY as this dose was previously shown to be sufficient for inhibition
340 of pRB signals (Yang et al, 2017). In mock-transfected cells this resulted in an almost complete
341 reduction of RB phosphorylation (**Fig. 4A,B**). We next tested cells transfected with Cyclin D3
342 alone, CDK6 alone, CDK6 co-transfected with Cyclin D3, and three CDK6 variants (the loss-of-
343 function variant D163N and above gain of function variants) also co-transfected with Cyclin D3
344 (**Fig. 4A,B**). Strikingly, we found that in the presence of LY overexpression of CDK6 induced pRB
345 levels significantly (~2.5-fold). Furthermore, co-expression of CDK6 with Cyclin D3 resulted in an
346 even greater increase by ~4.1-fold. Similar to our previous experiments, the S178P or R31C
347 variants produced comparable effects to CDK6. The D163N variant as expected showed low pRB
348 levels similar to control cells which demonstrates that effects of ectopic expression of
349 CDK6/Cyclin D3 are kinase-dependent and attributable to active CDK6. Whilst a single dose of
350 LY delivered the desired outcome of isolating CDK6 activity from the CDK4 background, we
351 additionally performed dose response curves (**Fig. 4C,D**). Whilst reduction of pRB levels at
352 increasing concentrations was observed in mock-transfected and Cyclin D3 overexpressing cells,
353 these levels were almost entirely sustained in cells transfected with CDK6/Cyclin D3. A similar
354 selection phenomenom was also observed using Ribociclib ([RI], LEE-011), another CDK4/6

355 inhibitor that is not chemically related to LY (Fassl *et al.*, 2022; Zhang et al., 2014)
356 (**Supplementary Fig. S2**). Overall, these results demonstrate that even in the absence of a
357 specific inhibitor CDK6 activity can be isolated in a convergent motif.

358

359 *In situ assay of CDK6 variants and modulators*

360 We have demonstrated through immunoblotting that CDK6 activity can be quantified in cells using
361 a combination of overexpression and CDK4/6 inhibition. We went on to test if this approach can
362 be applied in a high throughput compatible platform and in the exploration of the function of
363 engineered CDK6 variants. We employed an energy transfer-based assay to detect pRB (Ser780)
364 and total RB levels (**Fig. 5A**). This assay was chosen as it can be used with a greater efficiency
365 than immunoblotting. We first tested the same conditions as above and observed consistent
366 results. CDK6 and activating mutations displayed the greatest fold-increases in pRB levels
367 specifically in the presence of LY (e.g., a >6-fold difference in pRB levels compared to mock
368 inhibitor-treated cells; **Fig. 5A,B**). Also as observed earlier, CDK6 alone only showed a minor
369 increase and the two activating mutations overall behaved similarly.

370 Given the efficiency of this method, we applied it to study CDK6 function, inhibition and
371 regulation. We first tested whether LY-treated cells overexpressing CDK6/Cyclin D3 can be used
372 to screen for CDK6 inhibitors. Using RI as a test compound, we found that this is indeed the case
373 (**Fig. 5C**). We also examined genetically-engineered versions of CDK6. Fluorescent proteins are
374 commonly fused to enzymes as reporters of cellular levels/location or as functional regulators
375 (Bajar et al., 2016; Rodriguez et al., 2017; Zhou et al., 2017). These modifications can however
376 be associated with a negative impact on protein function (Patel et al., 2019; Snapp, 2009). We
377 introduced sequences encoding the photoactive pdDronpa1 protein (Zhou *et al.*, 2017) at two
378 separate sites of CDK6 to examine if insertion at either site alters activity. pdDronpa1 is a GFP-
379 like protein domain that has been previously used to generate photoswitchable (ps) kinases. Ps-
380 kinases, such as psCDK5, contain pdDronpa1 fused to the N-terminus and inserted in an internal
381 loop (Patel *et al.*, 2019; Zhou *et al.*, 2017). We introduced pdDronpa1 at the N-terminus of CDK6
382 as well as within an internal loop (located between helices α_F and α_G, homologous to insertion in
383 psCDK5 (Zhou *et al.*, 2017), **Supplementary Fig. S3**) as two separate constructs. We found that
384 the N-terminal insertion was well tolerated; however, insertion into the internal loop site completely
385 abolishes activity (**Fig. 5D**). Lastly, we explored the effects of protein modulators of CDK4/6
386 function by co-transfecting the INK4 inhibitor protein p18INK4c (p18). INK4 proteins are known to
387 specifically inhibit and modulate CDK4/6 activity by disrupting the cyclin interaction (Nebenfuehr
388 et al., 2020; Parry *et al.*, 1999). We transfected p18 alone or in combination with CDK6/Cyclin D3
389 or CDK6-R31C/Cyclin D3. The R31C mutant was included as it has previously been shown to
390 reduce binding of INK4 proteins to CDK6 (Hu *et al.*, 2011). Indeed, we found that p18 was able
391 to effectively inhibit CDK6 but unable to inhibit the R31C mutant (**Fig. 5E**). Overall, these findings
392 establish an assay to test genetically modified CDK6 variants and the effect of CDK6 modulators
393 on kinase activity.

394

395

396 **DISCUSSION**

397 The organization of biological systems into networks permits the emergence of complex functions
398 from a finite number of components and interactions. Kinase-substrate interactions have been
399 previously systematically analyzed towards inference of the global network and targeted
400 perturbation of disease-related network elements. The objectives of our study were more
401 reductionist as we focused on local motifs and functional *in situ* assays. Specifically, we
402 addressed three questions with respect to cKSRs. How common are cKSRs in experimentally

validated Ser/Thr and Tyr phosphorylation events? What are the most common motif topologies? And, for the prototypical convergent CDK4/6 kinase pair, how can individual kinases in the motifs be studied experimentally?

To answer the first two questions, we systematically mapped human phosphorylation reactions from the comprehensive PSP. We found that a large number of human substrates are phosphorylated by more than one kinase. Furthermore, a majority of human kinases participate in cKSRs, and for both Ser/Thr and Tyr kinases a wide variety of interaction stoichiometries can be observed. Finally, in many cases the kinases that act on a common substrate are co-expressed in a large fraction of analyzed cell models. This data collectively points to an abundance of convergent phosphorylation interactions that have the potential to drive multi-site phosphorylation events (associated with amplification, crosstalk and feedback) or redundant phosphorylation events (attributed as a source of diversity and robustness). Our analysis is novel and complementary to kinase-substrate enrichment analysis (Casado et al., 2013), which exploits known KSRs to quantify the strength of these interactions in samples under varying experimental conditions. The objective of our work was to identify the basic properties of cKSRs as a basis for further experimental exploration, as demonstrated here for CDK4/6.

To answer the third question, we studied the convergent CDK4/6 pair under conditions of kinase inhibition. ATP-competitive CDK4/6 inhibitors have led to major improvements in the survival of breast cancer patients. Resistance has emerged in the patient population and, albeit studied intensively, no resistance inducing kinase mutations or substrate protein mutations have been observed. In turn, resistance was attributed to upregulation of CDK6 levels (Cornell *et al.*, 2019; Li *et al.*, 2022; Li *et al.*, 2018; Yang *et al.*, 2017). We hypothesized that the interplay of expression level and drug sensitivity can also be explored to design an *in situ* assay for CDK6. We performed these experiments in cells expressing high levels of CDK4 to provide a test bed in which this second input entirely masks effects of initial CDK6 overexpression. Ultimately, the generated experimental strategy allowed us to quantify the activity of genetically modified kinases, small molecule inhibitors and inhibitory accessory proteins in living cells. The emerging assay complements existing assays of CDK6 that were in conducted *in vitro* (Bockstaele *et al.*, 2009; Li *et al.*, 2022; Soamalala *et al.*, 2020). It also opens the door to more rapid protein engineering approaches that require quantification of cellular CDK6 activity. For instance, we showed that unlike CDK5 (Zhou *et al.*, 2017), CDK6 is not amenable to internal pDronpa1 modification. The ability to perform these experiments with inhibitors from different chemical classes (as demonstrated here for LY and RI) allows separating off-target effects (e.g., from inhibition of upstream kinases). Several potential mechanisms for inhibitor resistance in CDK6-amplified cells have been proposed. In the first mechanism, kinases at elevated protein levels are not efficiently inhibited at tuned drug concentrations, and consequently differential signals are recorded between cells with low (e.g., WT cells) or high CDK6 levels (e.g., CDK6 overexpressing cells). In a second mechanism, resistance of CDK6 to small molecule inhibitors may be modulated by accessory proteins, including p18 (Li *et al.*, 2022). Our data suggest that the first mechanism is at play here as we observed a canonical inhibitory function of p18 in the presence of LY leading to reduced pRB levels.

Overall, we here analyzed phosphorylation maps using a convergence-centric approach and, in a prototypical experimental system, dissected convergence. Notably, latter experimental result was achieved even in the absence of specific inhibitors or knock-out cell models of the individual converging kinases. Similar limitations may apply to many other scenarios involving convergent kinases. We developed a cellular assay for CDK6 that is desirable as experiments in cells may reflect on a complex natural environment of enzymes and an impact of cellular environment on drug properties. Quite likely redundancy and convergence also exist in other post-translation modification networks, and our work may provide clues as to how to analyze these emerging phenomena.

ACKNOWLEDGEMENTS

We thank Q. Li and S. Chandarlapaty for advice on experimental design, M. Michael and D. Lynn for advice on databases and expression level analysis. This study was supported by grants of the Australian Research Council (FT200100519 and DP200102093, to H.J.), the National Health and Medical Research Council (APP1187638, to H.J.) and a PhD Top-up Scholarship by the Juvenile Diabetes Research Foundation Australia (to C.G.). The Australian Regenerative Medicine Institute is supported by grants from the State Government of Victoria and the Australian Government. The EMBL Australia Partnership Laboratory (EMBL Australia) is supported by the National Collaborative Research Infrastructure Strategy (NCRIS) of the Australian Government. MicroMon of Monash University provided Sanger sequencing services.

AUTHOR CONTRIBUTIONS

Conceptualization, C.G. and H.J.; Formal Analysis, R.S. and H.J.; Funding Acquisition, C.G. and H.J.; Methodology, C.G., R.S. and H.J.; Project Administration, H.J.; Investigation, C.G.; Data curation, C.G., R.S. and H.J.; Supervision, H.J.; Visualization, C.G. and H.J.; Writing - Original Draft, C.G. and H.J.; Writing - Review and Editing, H.J.

DECLARATION OF INTERESTS

The authors declare no competing interests.

Figures

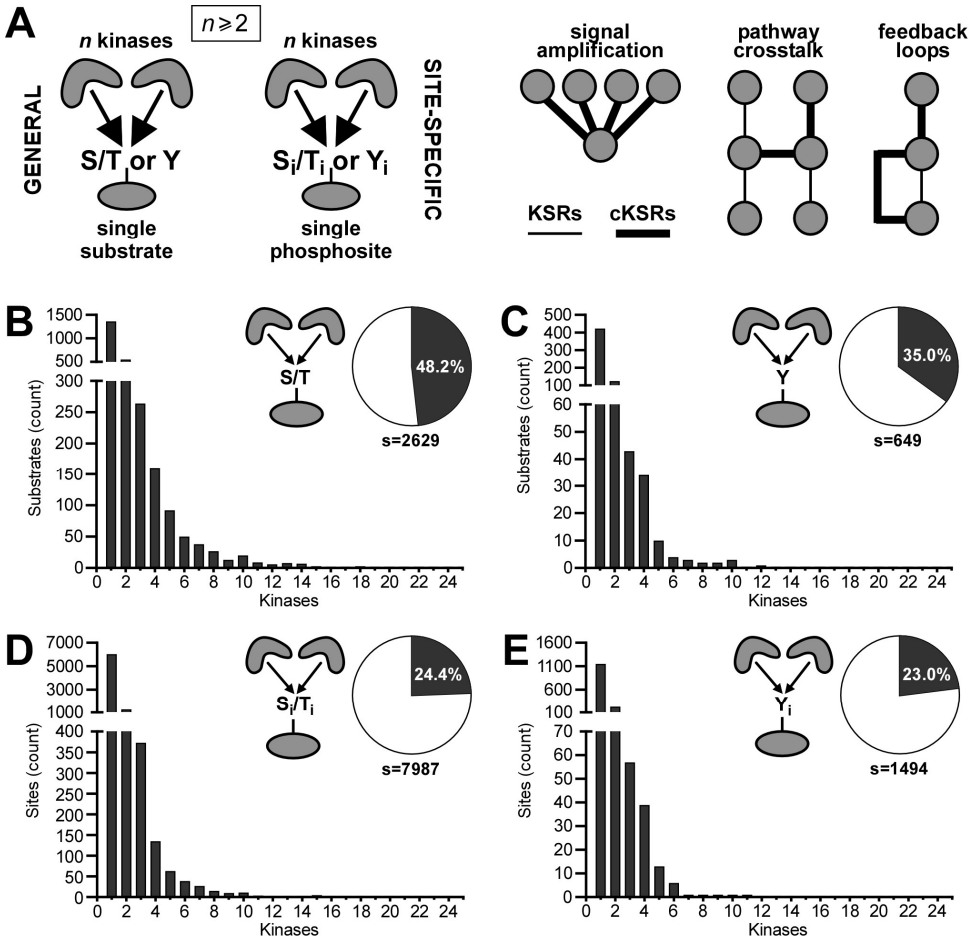

Figure 1: Substrate-centric analysis of convergent motifs for Ser/Thr and Tyr phosphorylation events. (**A**) cKSRs are defined as kinase-substrate interactions in which ≥two kinase phosphorylate a common substrate (general cKSRs) or a common site on a substrate (site-specific cKSRs). These interactions are involved in, e.g., convergence, pathway crosstalk and feedback loops. (**B,C**) Distribution histograms of general cKSRs for Ser/Thr phosphorylation (B) and Tyr phosphorylation (C). Bars indicate how many substrates are phosphorylated by the indicated number of kinases. Pie charts indicate the percentage of substrates that are phosphorylated by ≥two kinases and the total number of analyzed substrates (s). (**D,E**) Distribution histograms of site-specific cKSRs for Ser/Thr phosphorylation (D) and Tyr phosphorylation (E). Bars indicate how many sites are phosphorylated by the indicated number of kinases. Pie charts indicated the percentage of sites that are phosphorylated by ≥two kinases and the total number of analyzed sites (s).

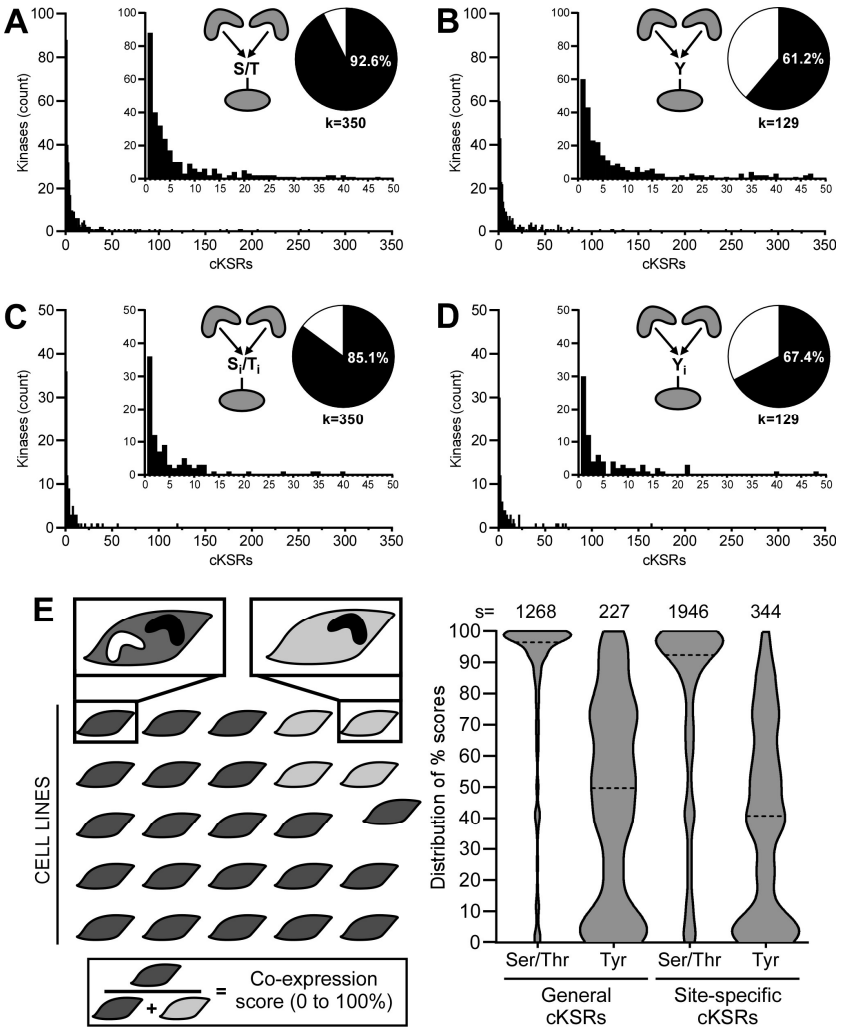

Figure 2: Kinase-centric analysis of convergent motifs for Ser/Thr and Tyr phosphorylation events. (**A,B**) Distribution histograms for Ser/Thr kinases (B) and Tyr kinases (C) in general cKSRs. Bars indicate how many kinases phosphorylate the indicated number of substrates. Pie charts indicate the percentage of kinases that participate in general cKSRs and the total number of kinases (k). (**C,D**) Distribution histograms for Ser/Thr kinases (B) and Tyr kinases (C) in site-specific cKSRs. Bars indicate how many kinases phosphorylate the indicated number of sites. Pie charts indicate the percentage of kinases that participate in site-specific cKSRs and the total number of kinases (k). (**E**) Co-expression analysis of converging kinases in cancer cell lines. For each group of kinases that phosphorylate the same substrate or site, the number of 1393 cancer cell lines that co-express these kinases was counted. From this, a co-expression score was calculated as the ratio of cells with (dark grey) and without (light gray) co-expression. Violin plots summarize the distribution of these scores for the analyzed number of substrates or sites (s) (dashed line: median; TPM threshold: 10).

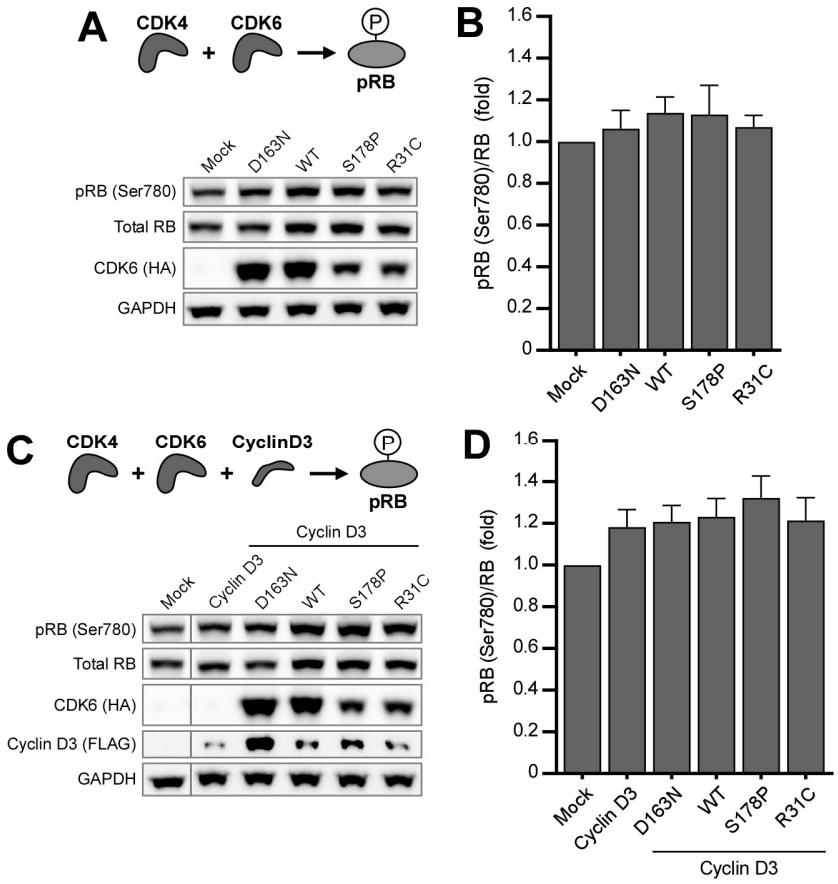

Figure 3: Overexpression of CDK6 and variants does not increase pRB levels. (**A**) Immunoblot analysis of pRB in MCF-7 cells expressing CDK6 and its variants. (**B**) Densitometry analysis of data shown in (A) expressed as a ratio of pRB to total RB. (**C**) Immunoblot analysis of pRB in MCF-7 cells expressing CDK6 and its variants when co-transfected with Cyclin D3. (**D**) Densitometry analysis of data shown (C) expressed as a ratio of pRB to total RB. (A and C) Representative experiments are shown. (B and D) n=3. Data are mean ± SEM.

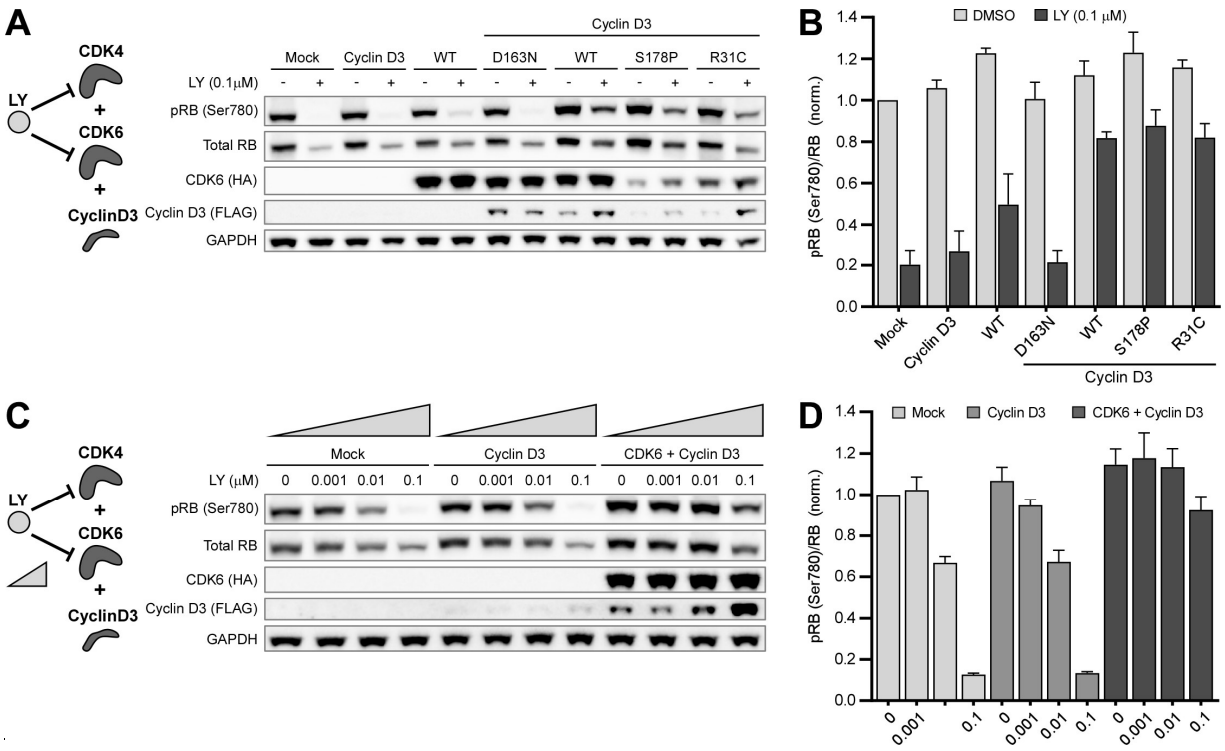

Figure 4: Kinase inhibition with LY reveals CDK6 activity. (**A**) Immunoblot analysis of pRB in MCF-7 cells expressing CDK6 and its variants when co-transfected with Cyclin D3, treated with LY or DMSO. (**B**) Densitometry analysis of data shown in (A) expressed as a ratio of pRB to total RB. (**C**) Immunoblot analysis of pRB in MCF-7 cells expressing CDK6 and Cyclin D3, treated with increasing concentrations of LY. (**D**) Densitometry analysis of data shown in (C) expressed as a ratio of pRB to total RB. (A and C) Representative experiments are shown. (B) n=4 and (C) n=3. Data are mean ± SEM.

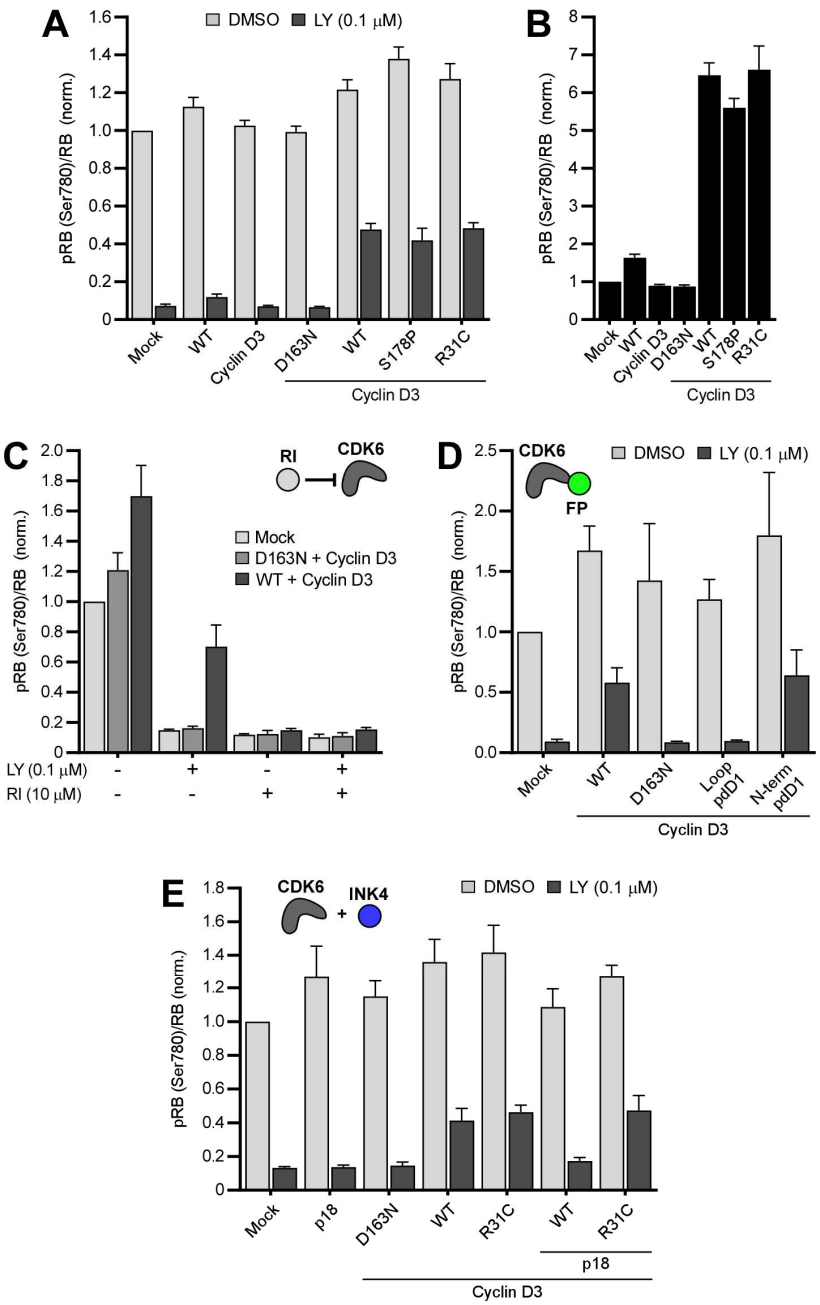

Figure 5: Energy transfer-based assay of CDK6 variants, inhibitors and modulators. (**A**) Ratios of pRB to total RB for MCF-7 cells expressing CDK6 and its variants co-transfected with Cyclin D3. (**B**) LY-treated conditions from (A) normalized to mock LY-treated control. (**C**) Ratios for cells expressing constructs and treated with different combinations of LY and RI. (**D**) Ratios for cells expressing CDK6 containing pdDronpa1 insertions within an internal loop (loop pdD1) or at the N-terminus (N-term pdD1). (**E**) Ratios for cells expressing $p18^{INK4c}$ (p18) in combination with CDK6 or R31C variant and Cyclin D3. (A-E) n=3. Data are mean ± SEM.

Supplementary Information

Supplementary Tables S1 to S8: Please see separate Excel files. These will be uploaded as Supplementary Data.

Supplementary Table S9: Protein sequences of WT CDK6 and engineered CDK6 variants. Color code: Start codon. HA tag. WT human CDK6. Linkers. pdDronpa1.

CDK6	MYPYDVPDYAEKDGLCRADQQYECVAEIGEGAYGKVFKARDLKNGGRFVALKRVRVQTGEEGMPLSTIREVAV LRHLETFEHPNVVRLFDVCTVSRTDRETKLTLVFEHVDQDLTTYLDKVPEPGVPTETIKDMMFQLLRGLDFLH SHRVVHRDLKPQNILVTSSGQIKLADFGLARIYSFQMALTSVVVTLWYRAPEVLLQSSYATPVDLWSVGCIFA EMFRRKPLFRGSSDVDQLGKILDVIGLPGEEDWPRDVALPRQAFHSKSAQPIEKFVTDIDELGKDLLLKCLTF NPAKRISAYSALSHPYFQDLERCKENLDSHLPPSQNTSELNTA
pdDronpa1-CDK6 (N-term pdD1)	MYPYDVPDYASVIKPDMKIKLRMEGAVNGHPFAIEGVGLGKPFEGKQSIDLKVKEGGPLPFAYDILTTAFCYG NRVFAKYPENIVDYFKQSFPEGYSWERSMNYEDGGICNATNDITLDGDCYIYEIRFRGTNFPANGPVMQKRTV KWEPSTENLYVRDGVLKGDVVMALSLEGGGHYRCDFKTTYKAKKVVQLPDYHFVDHHIEIKSHDKDYSNVNLH EHAEAHSELPRQAKGLKGSGEKDGLCRADQQYECVAEIGEGAYGKVFKARDLKNGGRFVALKRVRVQTGEEGM PLSTIREVAVLRHLETFEHPNVVRLFDVCTVSRTDRETKLTLVFEHVDQDLTTYLDKVPEPGVPTETIKDMMF QLLRGLDFLHSHRVVHRDLKPQNILVTSSGQIKLADFGLARIYSFQMALTSVVVTLWYRAPEVLLQSSYATPV DLWSVGCIFAEMFRRKPLFRGSSDVDQLGKILDVIGLPGEEDWPRDVALPRQAFHSKSAQPIEKFVTDIDELG KDLLLKCLTFNPAKRISAYSALSHPYFQDLERCKENLDSHLPPSQNTSELNTA
CDK6-internal-pdDronpa1 (loop pdD1)	MYPYDVPDYAEKDGLCRADQQYECVAEIGEGAYGKVFKARDLKNGGRFVALKRVRVQTGEEGMPLSTIREVAV LRHLETFEHPNVVRLFDVCTVSRTDRETKLTLVFEHVDQDLTTYLDKVPEPGVPTETIKDMMFQLLRGLDFLH SHRVVHRDLKPQNILVTSSGQIKLADFGLARIYSFQMALTSVVVTLWYRAPEVLLQSSYATPVDLWSVGCIFA EMFRRKPLFRGTGGSVIKPDMKIKLRMEGAVNGHPFAIEGVGLGKPFEGKQSIDLKVKEGGPLPFAYDILTTA FCYGNRVFAKYPENIVDYFKQSFPEGYSWERSMNYEDGGICNATNDITLDGDCYIYEIRFRGTNFPANGPVMQ KRTVKWEPSTENLYVRDGVLKGDVVMALSLEGGGHYRCDFKTTYKAKKVVQLPDYHFVDHHIEIKSHDKDYSN VNLHEHAEAHSELPRQAKRTSSDVDQLGKILDVIGLPGEEDWPRDVALPRQAFHSKSAQPIEKFVTDIDELGK DLLLKCLTFNPAKRISAYSALSHPYFQDLERCKENLDSHLPPSQNTSELNTA

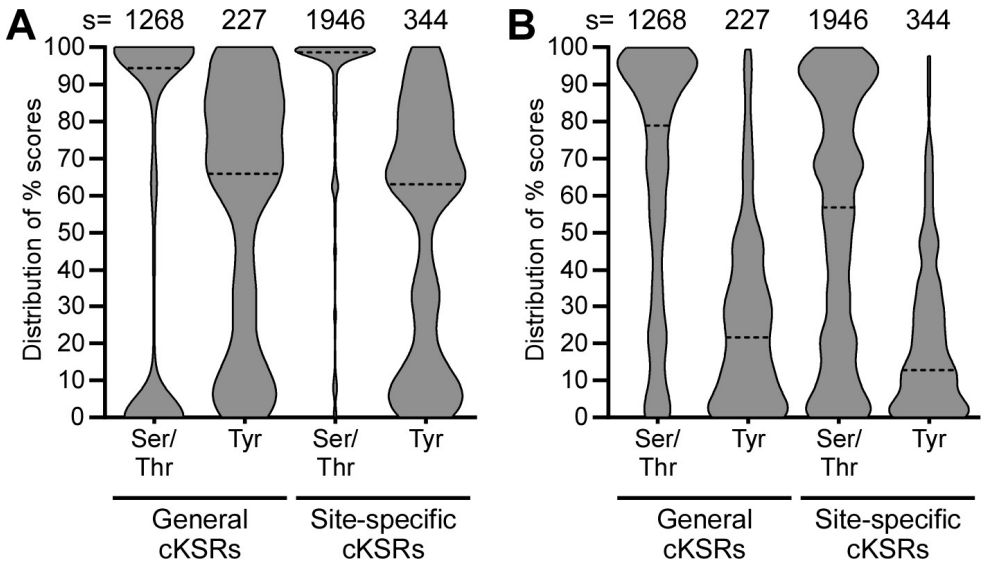

Supplementary Figure S1: Co-expression analysis at different TPM thresholds. (**A**) TPM threshold of 5. (**B**) TPM threshold of 20. Co-expression scores and median (dashed line) are defined as in Fig. 2. s: Analyzed number of substrates or sites.

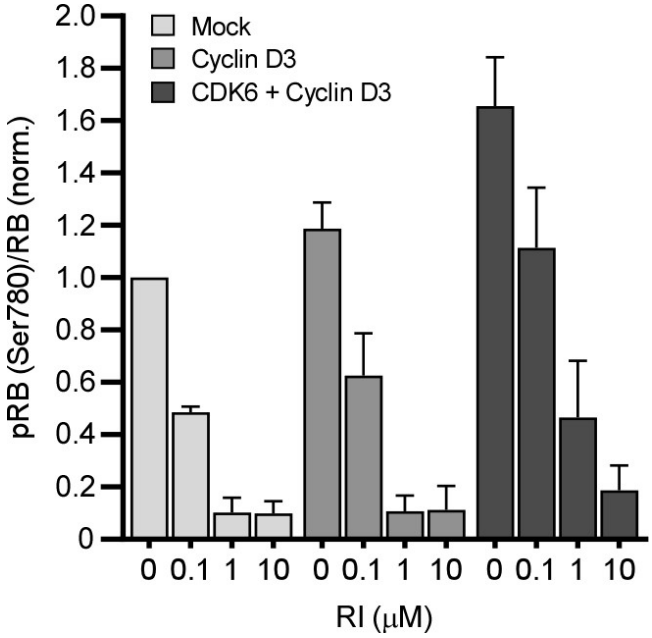

Supplementary Figure S2: Kinase inhibition with RI reveals CDK6 activity. Energy transfer-based assay to detect ratios of pRB to total RB for MCF-7 cells expressing CDK6 and Cyclin D3 treated with increasing concentrations of RI. n=3. Data are mean ± SEM.

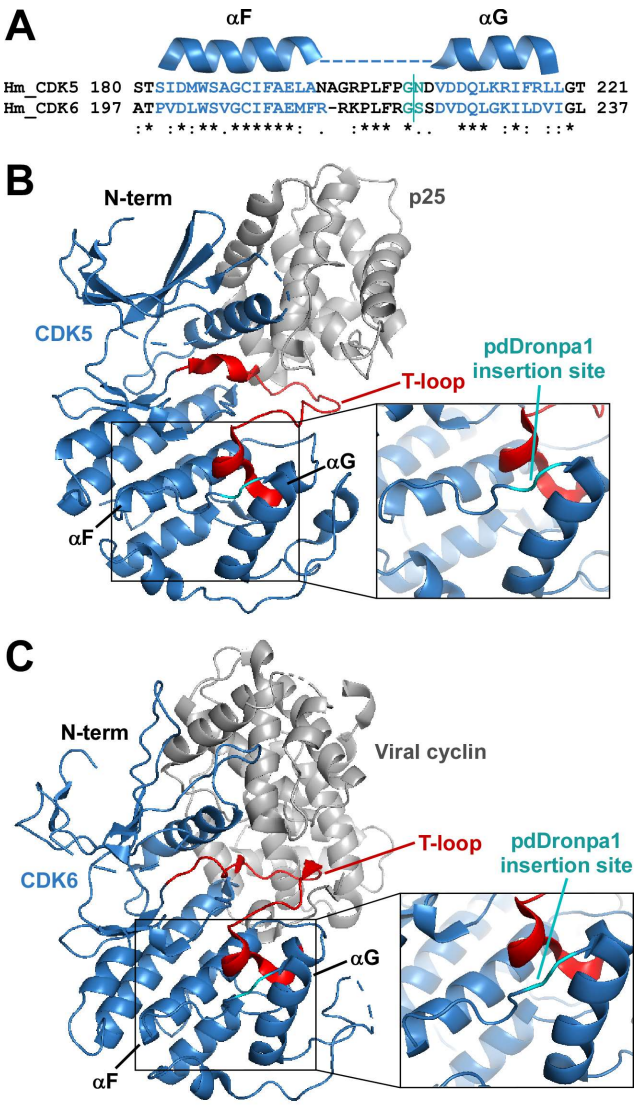

Supplementary Figure S3: Analogous insertion sites of pDronpa1 in CDK5 and CDK6. (**A**) Protein sequence alignment of human CDK5 and CDK6. pdDronpa1 internal loop insertion site highlighted in cyan (for CDK5, the insertion is equivalent to that of psCDK5 (Zhou *et al.*, 2017)). (**B** and **C**) CDK5-p25 and CDK6-viral cyclin complex structures with the insertion sites highlighted (PDB-IDs: 1H4L for CDK5 and 1JOW for CDK6).

556 **References**

557 Aebersold, R., and Mann, M. (2016). Mass-spectrometric exploration of proteome structure and
558 function. Nature *537*, 347-355.

559 Alganem, K., Hamoud, A.R., Creeden, J.F., Henkel, N.D., Imami, A.S., Joyce, A.W., Ryan, V.W.,
560 Rethman, J.B., Shukla, R., O'Donovan, S.M., et al. (2022). The active kinome: The modern view of
561 how active protein kinase networks fit in biological research. Curr Opin Pharmacol *62*, 117-129.

562 Anders, L., Ke, N., Hydbring, P., Choi, Y.J., Widlund, H.R., Chick, J.M., Zhai, H., Vidal, M., Gygi,
563 S.P., and Braun, P. (2011). A systematic screen for CDK4/6 substrates links FOXM1
564 phosphorylation to senescence suppression in cancer cells. Cancer Cell *20*, 620-634.

565 Bajar, B.T., Lam, A.J., Badiee, R.K., Oh, Y.-H., Chu, J., Zhou, X.X., Kim, N., Kim, B.B., Chung, M.,
566 and Yablonovitch, A.L. (2016). Fluorescent indicators for simultaneous reporting of all four cell cycle
567 phases. Nat Methods *13*, 993-996.

568 Barretina, J., Caponigro, G., Stransky, N., Venkatesan, K., Margolin, A.A., Kim, S., Wilson, C.J.,
569 Lehár, J., Kryukov, G.V., and Sonkin, D. (2012). The cancer cell line encyclopedia enables predictive
570 modelling of anticancer drug sensitivity. Nature *483*, 603-607.

571 Blain, S. (2008). Switching cyclin D-Cdk4 kinase activity on and off. Cell Cycle *7*, 892-898.

572 Bockstaele, L., Bisteau, X., Paternot, S., and Roger, P.P. (2009). Differential regulation of cyclin-
573 dependent kinase 4 (CDK4) and CDK6, evidence that CDK4 might not be activated by CDK7, and
574 design of a CDK6 activating mutation. Mol Cell Biol *29*, 4188-4200.

575 Bockstaele, L., Kooken, H., Libert, F., Paternot, S., Dumont, J.E., De Launoit, Y., Roger, P.P., and
576 Coulonval, K. (2006). Regulated activating Thr172 phosphorylation of cyclin-dependent kinase 4
577 (CDK4): its relationship with cyclins and CDK “inhibitors”. Mol Cell Biol *26*, 5070-5085.

578 Budde, A., Schneiderhan-Marra, N., Petersen, G., and Brüne, B. (2005). Retinoblastoma
579 susceptibility gene product pRB activates hypoxia-inducible factor-1 (HIF-1). Oncogene *24*, 1802-
580 1808.

581 Casado, P., Rodriguez-Prados, J.C., Cosulich, S.C., Guichard, S., Vanhaesebroeck, B., Joel, S.,
582 and Cutillas, P.R. (2013). Kinase-substrate enrichment analysis provides insights into the
583 heterogeneity of signaling pathway activation in leukemia cells. Sci Signal *6*, rs6.

584 Chen, P.L., Riley, D.J., Chen-Kiang, S., and Lee, W.H. (1996a). Retinoblastoma protein directly
585 interacts with and activates the transcription factor NF-IL6. Proc Natl Acad Sci U S A *93*, 465-469.

586 Chen, P.L., Riley, D.J., Chen, Y., and Lee, W.H. (1996b). Retinoblastoma protein positively
587 regulates terminal adipocyte differentiation through direct interaction with C/EBPs. Genes Dev *10*,
588 2794-2804.

589 Chen, Y.A., and Eschrich, S.A. (2014). Computational methods and opportunities for
590 phosphorylation network medicine. Transl Cancer Res *3*, 266-278.

591 Cheng, M., Olivier, P., Diehl, J.A., Fero, M., Roussel, M.F., Roberts, J.M., and Sherr, C.J. (1999).
592 The p21(Cip1) and p27(Kip1) CDK 'inhibitors' are essential activators of cyclin D-dependent kinases
593 in murine fibroblasts. EMBO J *18*, 1571-1583.

594 Colinge, J., César-Razquin, A., Huber, K., Breitwieser, F.P., Májek, P., and Superti-Furga, G. (2014).
595 Building and exploring an integrated human kinase network: global organization and medical entry
596 points. J Proteomics *107*, 113-127.

597 Cornell, L., Wander, S.A., Visal, T., Wagle, N., and Shapiro, G.I. (2019). MicroRNA-mediated
598 suppression of the TGF-β pathway confers transmissible and reversible CDK4/6 inhibitor resistance.
599 Cell Rep *26*, 2667-2680.e2667.

600 Dall'Acqua, A., Sonego, M., Pellizzari, I., Pellarin, I., Canzonieri, V., D'Andrea, S., Benevol, S., Sorio,
601 R., Giorda, G., Califano, D., et al. (2017). CDK6 protects epithelial ovarian cancer from platinum-
602 induced death via FOXO3 regulation. EMBO Mol Med *9*, 1415-1433.

603 Fassl, A., Geng, Y., and Sicinski, P. (2022). CDK4 and CDK6 kinases: From basic science to cancer
604 therapy. Science *375*, eabc1495.

605 Fisher, R.P. (2005). Secrets of a double agent: CDK7 in cell-cycle control and transcription. J Cell
606 Sci *118*, 5171-5180.

607 Gelbert, L.M., Cai, S., Lin, X., Sanchez-Martinez, C., Del Prado, M., Lallena, M.J., Torres, R.,
608 Ajamie, R.T., Wishart, G.N., and Flack, R.S. (2014). Preclinical characterization of the CDK4/6
609 inhibitor LY2835219: in-vivo cell cycle-dependent/independent anti-tumor activities alone/in
610 combination with gemcitabine. Invest New Drugs *32*, 825-837.

611 Hirai, H., Roussel, M.F., Kato, J.Y., Ashmun, R.A., and Sherr, C.J. (1995). Novel INK4 proteins, p19
612 and p18, are specific inhibitors of the cyclin D-dependent kinases CDK4 and CDK6. Mol Cell Biol *15*,
613 2672-2681.

614 Hornbeck, P.V., Zhang, B., Murray, B., Kornhauser, J.M., Latham, V., and Skrzypek, E. (2015).
615 PhosphoSitePlus, 2014: mutations, PTMs and recalibrations. Nucleic Acids Res *43*, D512-D520.

616 Hu, M.G., Deshpande, A., Schlichting, N., Hinds, E.A., Mao, C., Dose, M., Hu, G.-f., Van Etten, R.A.,
617 Gounari, F., and Hinds, P.W. (2011). CDK6 kinase activity is required for thymocyte development.
618 Blood *117*, 6120-6131.

619 Hydbring, P., Malumbres, M., and Sicinski, P. (2016). Non-canonical functions of cell cycle cyclins
620 and cyclin-dependent kinases. Nat Rev Mol Cell Biol *17*, 280-292.

621 Invergo, B.M., and Beltrao, P. (2018). Reconstructing phosphorylation signalling networks from
622 quantitative phosphoproteomic data. Essays Biochem *62*, 525-534.

623 Jinno, S., Hung, S.C., and Okayama, H. (1999). Cell cycle start from quiescence controlled by
624 tyrosine phosphorylation of Cdk4. Oncogene *18*, 565-571.

625 Kaelin, W.G., Jr. (1999). Functions of the retinoblastoma protein. Bioessays *21*, 950-958.

626 Kitagawa, M., Higashi, H., Jung, H.-K., Suzuki Takahashi, I., Ikeda, M., Tamai, K., Kato, J.-Y.,
627 Segawa, K., Yoshida, E., and Nishimura, S. (1996). The consensus motif for phosphorylation by
628 cyclin D1-Cdk4 is different from that for phosphorylation by cyclin A/E-Cdk2. EMBO J *15*, 7060-
629 7069.

630 Lemeer, S., and Heck, A.J. (2009). The phosphoproteomics data explosion. Curr Opin Chem Biol
631 *13*, 414-420.

632 Li, Q., Jiang, B., Guo, J., Shao, H., Del Priore, I.S., Chang, Q., Kudo, R., Li, Z., Razavi, P., and Liu,
633 B. (2022). INK4 tumor suppressor proteins mediate resistance to CDK4/6 kinase inhibitors. Cancer
634 Discov *12*, 356-371.

635 Li, Z., Razavi, P., Li, Q., Toy, W., Liu, B., Ping, C., Hsieh, W., Sanchez-Vega, F., Brown, D.N., and
636 Paula, A.F.D.C. (2018). Loss of the FAT1 tumor suppressor promotes resistance to CDK4/6
637 inhibitors via the hippo pathway. Cancer Cell *34*, 893-905. e898.

638 Lin, J., Jinno, S., and Okayama, H. (2001). Cdk6-cyclin D3 complex evades inhibition by inhibitor
639 proteins and uniquely controls cell's proliferation competence. Oncogene *20*, 2000-2009.

640 Malumbres, M. (2014). Cyclin-dependent kinases. Genome Biol *15*, 1-10.

641 Malumbres, M., and Barbacid, M. (2001). To cycle or not to cycle: a critical decision in cancer. Nat
642 Rev Cancer *1*, 222-231.

643 Malumbres, M., Sotillo, R.o., Santamaría, D., Galán, J., Cerezo, A., Ortega, S., Dubus, P., and
644 Barbacid, M. (2004). Mammalian cells cycle without the D-type cyclin-dependent kinases Cdk4 and
645 Cdk6. Cell *118*, 493-504.

646 Nebenfuehr, S., Kollmann, K., and Sexl, V. (2020). The role of CDK6 in cancer. Int J Cancer *147*,
647 2988-2995.

648 Parry, D., Mahony, D., Wills, K., and Lees, E. (1999). Cyclin D-CDK subunit arrangement is
649 dependent on the availability of competing INK4 and p21 class inhibitors. Mol Cell Biol *19*, 1775-
650 1783.

651 Patel, A.L., Yeung, E., McGuire, S.E., Wu, A.Y., Toettcher, J.E., Burdine, R.D., and Shvartsman,
652 S.Y. (2019). Optimizing photoswitchable MEK. Proc Natl Acad Sci U S A *116*, 25756-25763.

653 Paternot, S., Coulonval, K., Dumont, J.E., and Roger, P.P. (2003). Cyclic AMP-dependent
654 phosphorylation of cyclin D3-bound CDK4 determines the passage through the cell cycle restriction
655 point in thyroid epithelial cells. J Biol Chem *278*, 26533-26540.

656 Pellerano, M., and Morris, M.C. (2021). Fluorescent peptide biosensors for probing CDK kinase
657 activity in cell extracts. Methods Mol Biol *2329*, 39-50.

658 Riley, N.M., and Coon, J.J. (2016). Phosphoproteomics in the Age of Rapid and Deep Proteome
659 Profiling. Anal Chem *88*, 74-94.

660 Rodriguez, E.A., Campbell, R.E., Lin, J.Y., Lin, M.Z., Miyawaki, A., Palmer, A.E., Shu, X., Zhang, J.,
661 and Tsien, R.Y. (2017). The growing and glowing toolbox of fluorescent and photoactive proteins.
662 Trends Biochem Sci *42*, 111-129.

663 Rubin, S.M. (2013). Deciphering the retinoblastoma protein phosphorylation code. Trends Biochem
664 Sci *38*, 12-19.

665 Schachter, M.M., Merrick, K.A., Larochelle, S., Hirschi, A., Zhang, C., Shokat, K.M., Rubin, S.M., and
666 Fisher, R.P. (2013). A Cdk7-Cdk4 T-loop phosphorylation cascade promotes G1 progression. Mol
667 Cell *50*, 250-260.

668 Sherr, C.J., Beach, D., and Shapiro, G.I. (2016). Targeting CDK4 and CDK6: From discovery to
669 therapy. Cancer Discov *6*, 353-367.

670 Sherr, C.J., and Roberts, J.M. (1999). CDK inhibitors: positive and negative regulators of G1-phase
671 progression. Genes Dev *13*, 1501-1512.

672 Snapp, E.L. (2009). Fluorescent proteins: a cell biologist's user guide. Trends Cell Biol *19*, 649-655.

673 Soamalala, J., Diot, S., Pellerano, M., Blanquart, C., Galibert, M., Jullian, M., Puget, K., and Morris,
674 M.C. (2020). Fluorescent peptide biosensor for probing CDK6 activity in lung cancer cell extracts.
675 ChemBioChem.

676 Tigan, A., Bellutti, F., Kollmann, K., Tebb, G., and Sexl, V. (2016). CDK6—a review of the past and a
677 glimpse into the future: from cell-cycle control to transcriptional regulation. Oncogene *35*, 3083-3091.

678 Van, T.N.N., Pellerano, M., Lykaso, S., and Morris, M.C. (2014). Fluorescent protein biosensor for
679 probing CDK/cyclin activity in vitro and in living cells. ChemBioChem *15*, 2298-2305.

680 Wang, H., Nicolay, B.N., Chick, J.M., Gao, X., Geng, Y., Ren, H., Gao, H., Yang, G., Williams, J.A.,
681 and Suski, J.M. (2017). The metabolic function of cyclin D3–CDK6 kinase in cancer cell survival.
682 Nature *546*, 426-430.

683 Yang, C., Li, Z., Bhatt, T., Dickler, M., Giri, D., Scaltriti, M., Baselga, J., Rosen, N., and
684 Chandarlapaty, S. (2017). Acquired CDK6 amplification promotes breast cancer resistance to
685 CDK4/6 inhibitors and loss of ER signaling and dependence. Oncogene *36*, 2255-2264.

686 Zhang, Y.-X., Sicinska, E., Czaplinski, J.T., Remillard, S.P., Moss, S., Wang, Y., Brain, C., Loo, A.,
687 Snyder, E.L., and Demetri, G.D. (2014). Antiproliferative effects of CDK4/6 inhibition in CDK4-
688 amplified human liposarcoma in vitro and in vivo. Mol Cancer Ther *13*, 2184-2193.

689 Zhou, X.X., Fan, L.Z., Li, P., Shen, K., and Lin, M.Z. (2017). Optical control of cell signaling by
690 single-chain photoswitchable kinases. Science *355*, 836-842.